

Investigations Towards Tryptophan Uptake and Transport Across an In Vitro Model of the Oral Mucosa Epithelium

Grace C. Lin¹, Julia Tevini^{2,3}, Lisa Mair², Heinz-Peter Friedl¹, Dietmar Fuchs⁴, Thomas Felder³, Johanna M. Gostner² and Winfried Neuhaus^{1,5}

¹AIT – Austrian Institute of Technology GmbH, Competence Unit Molecular Diagnostics, Center for Health and Bioresources, Vienna, Austria. ²Medical University of Innsbruck, Biocenter, Institute of Medical Biochemistry, Austria. ³Paracelsus Medical University, Department of Laboratory Medicine, Salzburg, Austria. ⁴Medical University of Innsbruck, Biocenter, Institute of Biological Chemistry, Austria. ⁵Department of Medicine, Faculty of Medicine and Dentistry, Danube Private University, Krems, Austria.

International Journal of Tryptophan Research
Volume 17: 1–11
© The Author(s) 2024
Article reuse guidelines:
sagepub.com/journals-permissions
DOI: 10.1177/11786469241266312



ABSTRACT: Tryptophan is an essential amino acid and plays an important role in several metabolic processes relevant for the human health. As the main metabolic pathway for tryptophan along the kynurenine axis is involved in inflammatory responses, changed metabolite levels can be used to monitor inflammatory diseases such as ulcerative colitis. As a progenitor of serotonin, altered tryptophan levels have been related to several neurodegenerative diseases as well as depression or anxiety. While tryptophan concentrations are commonly evaluated in serum, a non-invasive detection approach using saliva might offer significant advantages, especially during long-term treatments of patients or elderly. In order to estimate whether active transport processes for tryptophan might contribute to a potential correlation between blood and saliva tryptophan concentrations, we investigated tryptophan's transport across an established oral mucosa in vitro model. Interestingly, treatment with tryptophan revealed a concentration dependent secretion of tryptophan and the presence of a saturable transporter while transport studies with deuterated tryptophan displayed increased permeability from the saliva to the blood compartment. Protein analysis demonstrated a distinct expression of L-type amino acid transporter 1 (LAT1), the major transporter for tryptophan, and exposure to inhibitors (2-amino-2-norbornanecarboxylic acid (BCH), L-leucine) led to increased tryptophan levels on the saliva side. Additionally, exposure to tryptophan in equilibrium studies resulted in a regulation of LAT1 at the mRNA level. The data collected in this study suggest the participation of active transport mechanisms for tryptophan across the oral mucosa epithelium. Future studies should investigate the transport of tryptophan across salivary gland epithelia in order to enable a comprehensive understanding of tryptophan exchange at the blood-saliva barrier.

KEYWORDS: Tryptophan, diagnostics, oral mucosa, inflammatory diseases, TR146

RECEIVED: January 5, 2024. **ACCEPTED:** June 3, 2024.

TYPE: Original Research Article

FUNDING: The author(s) received no financial support for the research, authorship, and/or publication of this article.

DECLARATION OF CONFLICTING INTERESTS: The author(s) declared no potential conflicts of interest with respect to the research, authorship, and/or publication of this article.

CORRESPONDING AUTHOR: Winfried Neuhaus, AIT – Austrian Institute of Technology GmbH, Competence Unit Molecular Diagnostics, Center for Health and Bioresources, Giefinggasse 4, Vienna 1210, Austria. Email: winfried.neuhaus@ait.ac.at

Introduction

Tryptophan (Trp), an essential neutral amino acid, plays an important role in the regulation of metabolic processes functions for immunity and neuronal function as well as intestinal homeostasis.¹ Trp is mainly (>95%) metabolized by the kynurenine (Kyn) pathway in humans and also serves as the precursor for the neurotransmitter serotonin.^{2,3} Trp is catalysed by indoleamine 2,3-dioxygenases (IDO)-1 and -2 or tryptophan-2,3-dioxygenase (TDO) to Kyn. As the IDO-1-dependent Trp route is upregulated in response to inflammation, the Kyn pathway plays a major role in inflammatory conditions.³ Studies have shown a dysregulated Trp metabolism in ulcerative colitis⁴ and associated reduced serum levels of Trp with bowel diseases.⁵ Additionally, obesity in adults displayed altered Trp metabolism showing a higher Kyn to Trp ratio (Kyn/Trp).⁶ As Trp is also substrate for synthesis of serotonin,² neurodegenerative diseases have been linked to a dysfunctional metabolism or depletion of Trp.^{7,8}

Trp transport is catalysed by the L-type amino acid transporter 1 (LAT1, SLC7A5), a member of the amino acid-polyamine-organocation (APC) superfamily. LAT1 functions as an antiporter and mediates the influx/efflux of neutral amino acids and glutamine in a sodium (Na⁺)- and pH-independent manner.^{9,10} As cancer cells overexpress LAT1 to fuel nutritional demands, regulation of LAT1 serves as one of the therapeutic targets for drug development.¹¹ LAT1 forms a heterodimeric complex with the membrane glycoprotein 4F2hc (also known as CD98, SLC3A2).⁹ Even though extensive structural analysis of the complex was performed,⁹ the mechanism remains unclear with regard to the involvement of 4F2hc in the transport process.

With Trp playing major roles in several metabolic processes and its concentration being directly linked to the activation of inflammatory responses and/or cognitive functions, the evaluation of Trp levels in patients provides advantages of monitoring of a relevant biomarker. While Trp is commonly analysed in serum, the process of blood drawing is often associated with



discomfort for the patient. Hence, a non-invasive sampling approach via saliva to assess Trp levels would be advantageous to increase the flexibility and ease of sample collection. While the transport of biomarkers or molecules from blood to saliva is limited by epithelial layers of the salivary glands and oral mucosa (also called the blood-saliva barrier), several serum biomarkers have been found to correlate with salivary biomarkers concentration. Advances in diagnostic methods in recent years led to an improved understanding of saliva composition with, for instance, levels of salivary C-reactive protein (CRP) as biomarker associated with systemic inflammation.^{12,13}

To assess the potential of Trp as a salivary biomarker, we used an established and thoroughly characterized oral mucosa model of the blood-saliva barrier to analyse its transport from blood to saliva or *vice versa*. The model based on TR146 cells has been thoroughly validated on its cellular expression of transporters, tight junctions and keratin markers among others, and more importantly has confirmed to build a paracellular barrier, verified by transepithelial electrical resistance (TEER) measurements and transport of the paracellular marker carboxyfluorescein.¹⁴ Recently, the oral mucosa model was used to investigate the transport direction and mechanism of salivary biomarkers, such as CRP¹⁵ and ferritin¹⁶ and has proven to provide a reliable *in vitro* model for this purpose. In this study, we investigated the uptake and transport of Trp in the oral mucosa model and demonstrated a role of LAT1 for Trp uptake.

Methods

Cell culture

The human buccal carcinoma cell line TR146 was purchased from Sigma-Aldrich (St. Louis, MO, US, 10032305) and cultivated in Dulbecco's Modified Eagle Medium (DMEM, Sigma-Aldrich, St. Louis, MO, US, D5796), supplemented with 10% Fetal Calf Serum (FCS, Sigma-Aldrich, St. Louis, MO, US, F9665) and 1% Penicillin/Streptomycin (Pen/Strep, Merck, Darmstadt, Germany, A2213) in T25 TC treated cell culture flasks (Greiner, Bio-One GmbH, Kremsmünster, Austria, CELLSTAR®, 690175) at 37°C, 5% CO₂, 95% air atmosphere and 95% humidity.

Cells were propagated weekly at a concentration of 9.33×10^3 cells/cm² with media change every 2 to 3 days. For equilibrium and transport studies cells from passage 5 to 45 were seeded on 24-well ThinCerts (Greiner, Bio-One GmbH, Kremsmünster, Austria, 662641) in 24-well plates (Greiner, Bio-One GmbH, Kremsmünster, Austria, 662160) with 900 µL media provided in the basolateral compartment and 300 µL cell suspension (4.8×10^4 cells/mL in media) in the apical compartment. As soon as cells reached confluency, cultivation was switched to airlift, and basolateral media was supplemented with 1% Human Keratinocytes Growth Factor (HKGS, ThermoFisher Scientific, Waltham, MA, US, S0015).

Cells were used for experiment after 3 weeks of airlift cultivation (cultivation described in more detail in Lin et al.¹⁴)

Equilibrium studies

On day of experiments, transepithelial electrical resistance (TEER) of cultivated cells was measured as described in Lin et al.¹⁴ in cultivation media and subsequently in amino-acid free Hank's Balanced Salt Solution (HBSS, Sigma-Aldrich, St. Louis, H6648) after 2 washing steps with HBSS. TEER values ($\Omega \times \text{cm}^2$) were calculated using the ohmic resistance values displayed as Ω upon measurement with Millicell ERS-1 Voltmeter (Merck, Darmstadt, Germany, MERS00001) and multiplied with the surface area of the membrane after subtraction of mean values from blanks without cells.

L-tryptophan (Trp, Sigma-Aldrich, St. Louis, T8941), L-leucine (Leu; Sigma-Aldrich, St. Louis, L8912) and 2-amino-2-norbornanecarboxylic acid (BCH, Sigma-Aldrich, St. Louis, A7902) were diluted in HBSS to a stock concentration of 5 mM, sterile filtered with 0.22 µm filters (Roth, P666.1) and stored at -20°C until further usage. Stock solutions were freshly diluted at start of experiments to 1, 3 and 10 µM (Trp) or 10, 100 and 1000 µM (Leu, BCH) in HBSS. Cells were treated either with HBSS alone (control) or respective solutions on the apical (300 µL) and basolateral (900 µL) compartment at 37°C. Additionally, blanks (ThinCerts without cells) were treated with Trp solutions on both sides for comparison. Samples from the apical and basolateral compartments were collected after 2, 6 or 21 hours and stored at -80°C until HPLC-FLD measurements. For each biological sample, cells from 2 separate ThinCerts were lysed and pooled together with 350 µL lysis buffer (RA1 buffer from NucleoSpin RNA Kit [Machery Nagel, 740961] supplemented with 1% β-mercaptoethanol) as one sample and stored at -80°C prior to RNA isolation.

Transport studies

Deuterated Trp (d5-Trp, dTrp, Santa-Cruz, Heidelberg, Germany, sc-475629) was dissolved to prepare a stock concentration of 3 mM in HBSS and sterile filtered prior to usage. Stock solutions were diluted to 10 and 100 µM dTrp in fresh HBSS on day of experiment and applied on cells and blanks after TEER measurements. The dTrp solution with desired concentration was applied on the apical side for transport from the apical side to the basolateral side (A/B) or on the basolateral side for transport from the basolateral to the apical compartment (B/A). Apical (300 µL) or basolateral (900 µL) samples were collected and replaced with the same volume of fresh HBSS after 30 (t1), 90 (t2) and 210 minutes (t3). Samples were taken 450 minutes (t4) after the start of the experiment from the apical and basolateral compartments and stored at -80°C until analysis with HPLC-FLD and LC-MS/MS.

Permeability was calculated as shown below for transport from A/B. First, the cleared volume at each timepoint was calculated by multiplying the concentration in the basolateral compartments (C_{baso}) measured at the corresponding timepoint with the basolateral Volume (V_{baso}) and dividing by the applied stock concentration (C_{stock}) after subtraction of the basolateral concentration volume of the preceding timepoints, if applicable, under consideration of the volume ratio between the apical and basolateral compartments.

The total cleared volume was further plotted against the time to give the slope (PS), which was divided by the area (A) of the insert to result in the permeability (PE) of Trp.

$$\text{Cleared } V_{t_{i+n}} [\mu\text{L}] = \frac{C_{\text{baso}, t_{i+n}} [\mu\text{M}] * V_{\text{baso}} [\mu\text{L}]}{C_{\text{stock}} [\mu\text{M}] - \sum \left(C_{\text{baso}, (t_{i+n-1})} * 3 - \dots - C_{\text{baso}, i} * 3 \right) [\mu\text{M}]}$$

$$\text{Total cleared } V_{t_{i+n}} [\mu\text{L}] = \text{Cleared } V_{t_i} [\mu\text{L}] + \sum \text{Cleared } V_{t_{i+n-1}} [\mu\text{L}]$$

$$\text{PS}_{t_i-t_4} \left[\frac{\mu\text{L}}{\text{min}} \right] = \frac{\Delta \text{Total cleared } V_{t_i-t_4} [\mu\text{L}]}{\Delta t_{1-4} [\text{min}]}$$

$$\text{PE}_{t_i-t_4} \left[\frac{\mu\text{m}}{\text{min}} \right] = \frac{\text{PS}_{t_i-t_4} \left[\frac{\mu\text{m}^3}{\text{min}} \right]}{A_{\text{insert}} [\mu\text{m}^2]}$$

Cells were pooled with 350 μL lysis buffer as described above and stored at -80°C for RNA isolation.

HPLC-FLD measurements

Chemicals and reagents. Acetic acid, sodium acetate, trichloroacetic acid, Trp (T0254), Kyn (K8625) and 3-nitro-L-tyrosine were obtained from Sigma Aldrich (Vienna, Austria). Albumin was obtained from Serva (Heidelberg, Germany; 11922)

Calibrators and sample preparation. Calibrators for Trp and Kyn were prepared in water containing 7% (w/v) albumin and 0.9% (w/v) NaCl. 100 μL of calibrators or samples were mixed with 100 μL of the internal standard 3-nitro-L-tyrosine (25 $\mu\text{mol/L}$) and then precipitated with 25 μL trichloroacetic acid (2 mol/L). After centrifugation at 9500 $\times g$ for 6 minutes at room temperature the supernatant was collected and transferred into microvials for HPLC measurements.

HPLC-FLD analysis. In brief, chromatographic separation was carried out on a Varian ProStar 210 system (Varian Inc., Palo Alto, California) using a Purospher STAR RP-18 end-capped (3 μm) LiChroCART 55-4 column (Merck, Darmstadt, Germany) and 15 mM acetic acid – sodium acetate (pH

4.0) as the mobile phase (isocratic elution, flow rate of 0.9 mL/min), as described earlier.^{17,18} Sample injection was controlled by a Varian ProStar 410 autosampler. A Varian ProStar 360 fluorescence detector and a UV-detector (SPD-6A, Shimadzu) were used to detect Trp by its native fluorescence at 286 nm excitation and 366 nm emission wavelengths and kynurenic acid and 3-nitro-L-tyrosine by UV-absorption at 360 nm.

LC-MS/MS measurements

Chemicals and reagents. Acetonitrile (ACN, LC-MS grade, 83640.290), methanol (MeOH, LC-MS grade, 1.06035.1000), water (LC-MS grade, 83645.290) and formic acid (FA, >99%, 84865.180) were obtained from VWR International (Vienna, Austria). Trp and butylated hydroxy toluene (BHT, W218405) were purchased from Sigma-Aldrich (Vienna, Austria). Isotopically labeled dTrp (sc-475629) and d5-kynurenic acid (sc-470916) were obtained from Santa Cruz Biotechnology (Heidelberg, Germany).

Calibrators, quality controls and sample preparation. Calibrators for Trp and dTrp with concentrations of 0.08, 0.4, 2.0, 4.0, 20 and 100 $\mu\text{g/mL}$ as well as quality control samples (QCs) with concentrations of 0.4 and 20 $\mu\text{g/mL}$ Trp and dTrp were prepared in water containing 7% (w/v) albumin and 0.9% (w/v) NaCl. For sample preparation, 1% (v/v) FA and 8 volumes of cold MeOH including deuterated standard (d5-kynurenic acid, 0.08 $\mu\text{g/mL}$) and 0.05% BHT were added. After an incubation step for 30 minutes at -20°C , precipitates were centrifuged (10 minutes, 9500g, 4°C). The supernatant was transferred into a new Eppendorf tube and dried in the SpeedVac Vacuum Concentrator at 45°C for 2 hours. Samples were then resuspended in water containing 1% mobile phase B.

LC-MS/MS analyses. Trp and dTrp were quantified as described by Fuertig et al¹⁹ with minor modifications. Samples were processed on the day of measurement and kept in the autosampler at 4°C before quantification. Chromatographic separation was carried out on an Agilent 1200 series quaternary HPLC system (Böblingen, Germany) using a Chromolith Performance RP18-e column (100 \times 3 mm, Sorbent Lot/Column No.U120150/039) from Merck (Darmstadt, Germany) at a temperature of 20°C with water containing 0.5% FA as mobile phase A and 95/5 (vol/vol) acetonitrile/water containing 0.5% FA as mobile phase B. Gradient elution at a flow rate of 0.65 mL/min consisted of an isocratic step of 15.0% B for 0.2 minutes, from 15.0% to 95.0% B in 6.7 minutes, followed by a flushing step with 95.0% B for 1.5 minutes and an equilibration step with 15.0% B for 2.6 minutes. Total time for a single chromatographic run was 11.0 minutes. Selected reaction monitoring (SRM) measurements for metabolites as well as for the internal standards in obtained samples were performed on an API 4000 LC-MS/MS system (Sciex, Darmstadt, Germany) in positive ionization mode. Quantifier and qualifier

mass transitions m/z were 205.1/118.1 and 205.1/146.2 (Trp), 210.2/192.1 and 210.2/150.0 (dTrp) and 195.1/149.1 and 195.1/121.2 (d5-kynurenic acid), respectively. Analyst software 1.6.2 (Sciex, Darmstadt, Germany) was used for detection, analysis and quantification of data. Additional mass spectrometric parameters were set as follows: source temperature of 650°C, collision gas of 12 (AU), curtain gas of 15 (AU), ion source gas 1 of 60 (AU), ion source gas 2 of 50 (AU), ion spray voltage of 5200 V and entrance potential of 10 V. Inter-day and intraday accuracy coefficient of variation were 10.7% and 6.5% for low level QC ($n=6$). Calibration curves were derived from ratios of the analyte peak areas and the internal standards using 1/x-weighted linear least-squares regression of the area ratio versus the concentration of the corresponding internal standard.

Immunofluorescence staining

Microscopic slides (A. Hartenstein GmbH, Würzburg, Germany; DKR0, 10 × 10 mm) were disinfected with 500 µL/well 70% ethanol (EtOH) in 24-well plates for 45 minutes. Prior to coating with 300 µL 0.5% gelatine (w/v in dd-H₂O)/well for 30 minutes at room temperature, slides were washed twice with 500 µL PBS (Thermo Fisher, Waltham, MA, US; 1976785). TR146 cultivated in serum-free EpiLife (detailed preparation of media described in Lin et al¹⁴) were seeded at a cell density of 2.79×10^3 cells/cm² at passage 47 with media change every 2 to 3 days. Permeabilization with MeOH and subsequent washing steps was performed as described earlier.¹⁶ Staining was performed with primary antibody (SLC7A5, Abcam, ab85226, rabbit) diluted 1:100 in 1% Bovine Serum Albumin (BSA, Carl Roth; 8076.2)/PBS. After the incubation period and washing steps secondary antibody anti-rabbit IgG Alexa Fluor 488 (A-21206, Life technologies, donkey) was added at a dilution of 1:200 in 1% BSA/PBS. Upon washing steps and staining with DAPI (Sigma-Aldrich, St. Louis, MO, US; D9542), microscopic slides were embedded with Fluoprep (bioMerieux, 75521). Imaging was performed with the Zeiss Axio Observer.Z1 equipped with the Colibri LED illumination system and controlled by the software AxioVision Release 4.8.2.

TR146 were seeded in DMEM supplemented with 10% FCS and 1% Pen/Strep at passage 16 for staining on 24-well ThinCerts and were cultivated as described previously.¹⁴ Images was taken with an Olympus IX83 microscope equipped with a SOLA-SM LED Light Engine (Lumencor, Beaverton, OR, US), controlled by CellSens Software. Processing of the images was performed with OlyVIA Software 2.9 (Olympus, Vienna, Austria).

Western blot

For protein analysis TR146 were seeded on 6-well plates (Falcon, 353502) passage 16 at a cell density of 9.33×10^3 cells/

cm² in 3 mL DMEM supplemented with 10% FCS and 1% Pen/Strep per well. Media change was performed every 2 to 3 days until confluency was reached on day 8. Cells were either washed twice with DMEM supplemented with 1% Pen/Strep (DMEM w/o FCS) or HBSS and subsequently incubated in DMEM w/o FCS or HBSS for 24 hours at 37°C. For control samples media changes was performed simultaneously with DMEM supplemented with 1% Pen/Strep and 10% FCS. Sample collection was described in Lin et al¹⁵ previously. Briefly, cell layers were washed twice with 1 mL/well pre-cooled PBS on ice following an incubation for 5 minutes in PBS on ice. For lysis 50 µL RIPA buffer (1M Tris at pH 8, 150 mM NaCl, 0.1% SDS and 1% NP40-Substitute in dd-H₂O) supplemented with protease and phosphatase inhibitors (Roche, Basel, Switzerland, 05892970001 and 04906837001) was added for 30 minutes on ice. Protein samples were harvested by means of cell scrapers, and protein concentration was determined with the Pierce BCA assay kit (Thermo Fisher, Scientific, Waltham, MA, US, 23227) according to the manufacturer's instructions.

For Western blot analysis, 20 µg protein per sample were prepared with 4× Laemmli buffer (Bio-Rad, 161-0747) containing 10% β-mercaptoethanol for 5 minutes at 95°C and loaded on a 10% SDS-PAGE gel. Upon transferring the gel to a PVDF membrane (Bio-Rad, 162-0177) in the cool room overnight, the membrane was incubated in 5% skim milk (AppliChem Panreas, A0830,0500) for 2 hours at room temperature. After washing twice with 0.1% Tween20/PBS (PBST, Sigma, P7949, Gibco 18912-014) the primary antibody for SLC7A5 (Abcam, ab85226, rabbit diluted 1:250 in 5% skim milk) was added overnight at 4°C under gentle shaking. The membrane was washed 3 times with PBST for 10 minutes upon incubating with the HRP-labeled anti-mouse antibody (Sigma-Aldrich, St. Louis, MO, US, A3854, 7076S, 1:20 000 in 5% skim milk) for 1 hour at room temperature. Subsequently the membrane was incubated in ECL (Bio-Rad, 170-5060) for 5 minutes and bands were captured with ChemiDoc Imaging System (Bio-Rad).

For analysis of β-actin, the membrane was heated at 50°C in stripping buffer (dd-H₂O with 2% SDS, 1.25% of 0.5 mM TrisHCl pH 6.8 and 0.08% β-mercaptoethanol) for 45 minutes. Following rinsing in dd-H₂O for 1 hour, the membrane was washed once with PBST for 5 minutes and blocked with 5% skim milk for 1.5 to 2 hours at room temperature. After a washing step with PBST for 10 minutes, the membrane was incubated with the HRP labeled β-actin antibody (Sigma-Aldrich, A3854, 1:20 000 in 5% skim milk) for 1 hour at room temperature. Upon 3 washings steps for 10 minutes each with PBST, ECL was added for labeling and incubated for 5 minutes.

Images were captured with ChemiDoc Imaging system, analysis was performed with ImageLab Software Version 5.2.1 (Bio-Rad, Berkeley, CA, US).

Quantitative real-time PCR

RNA was isolated using the NucleoSpin RNA Kit (Machery Nagel, 740961) according to the manufacturer's instruction and eluted with 40 μ L nuclease-free water (Invitrogen, AM9937). For cDNA synthesis 1000 ng RNA was applied using the Multiscribe Reverse Transcriptase Kit (Applied Biosystem Thermo Scientific, 4311235). Quantitative real-time PCR was performed and analysed as described previously.¹⁵ Primers for 18SrRNA (forward 5'-3' ATGGTTCCTTTGGTCGCTCG, reverse 5'-3' GAGCTCACCGGGTTGGTTTT) and LAT1 (forward 5'-3' CGGCACCACCATCTCCAAAT, reverse 5'-3' AGCAGCAGCACGCAGAG) were used. For analysis, Δ Ct values of treated samples were normalized to Δ Ct values of control samples using the $2^{-\Delta\Delta C_t}$ method.

Statistical analysis

The results are shown as mean \pm standard deviation (SD). Sample size is indicated as N. Graphs and statistical analysis were illustrated or performed with SigmaPlot 14.0. Statistical analysis was performed as Student's *t*-test and two- or three-way ANOVA followed by post-hoc Holm-Sidak test with $\alpha = .05$, $P < .05$ indicated as *, $P < .01$ indicated as **, $P < .001$ indicated as ***.

Results

Equilibrium studies reveal saturable processes for tryptophan concentrations in the salivary compartment

After measuring TEER values ($214.14 \pm 117.38 \Omega \times \text{cm}^2$) to confirm barrier integrity, cells were treated with 0, 1, 3, 10 μ M Trp in HBSS on the apical and basolateral compartment. Trp concentrations were measured after 2, 6 and 21 hours revealing an increase of Trp in both compartments overtime (Figure 1). Kyn measurement of the samples showed concentrations lower than the detection limit ($<0.1 \mu\text{M}$). Interestingly, Trp concentrations in the basolateral compartment remained similar over time, while significantly higher concentrations were determined on the apical side (Figure 1B₁-D₁). In detail, cells treated with 1 μ M Trp reached apical concentrations 9.1-fold ($7.02 \pm 1.20 \mu\text{M}$) of applied stock concentrations ($0.77 \pm 0.14 \mu\text{M}$), while treatment with 3 μ M Trp resulted in apical concentrations 4.3-fold ($11.11 \pm 1.76 \mu\text{M}$) of applied stock concentrations ($2.58 \pm 0.54 \mu\text{M}$) after 21 hours. On the other hand, exposure to 10 μ M Trp only showed an increase of 1.61-fold ($13.36 \pm 0.84 \mu\text{M}$) on the apical side compared to stock concentrations ($8.31 \pm 1.04 \mu\text{M}$) after 21 hours. In comparison, Trp on the basolateral side after treatment with 1, 3 and 10 μ M Trp for 21 hours were measured as 3.03-fold ($2.34 \pm 0.40 \mu\text{M}$), 1.92-fold ($4.69 \pm 1.14 \mu\text{M}$) and 1.17-fold ($9.73 \pm 1.07 \mu\text{M}$) of applied stock solutions.

However, blanks (ThinCerts without cells) treated with Trp stock solutions apically and basolaterally showed no

significantly changed concentration after 21 hours in either compartments (Figure S1) supporting that cells secreted Trp over time. Indeed, Trp concentrations of untreated control cells in amino acid-free HBSS (0 μ M Trp) revealed Trp concentrations of $8.60 \pm 1.57 \mu\text{M}$ in the apical compartment and $1.98 \pm 0.62 \mu\text{M}$ in the basolateral compartment after 21 hours (Figure 1A).

Hence, to estimate the relation of secreted Trp to the applied stock concentration, measured Trp concentrations from controls (0 μ M Trp) were subtracted from measured values for each time point and normalized to the applied stock concentration in each experiment as x-fold (Figure 1B₂-D₂).

This correction revealed that Trp levels decrease with increasingly added Trp concentrations in the apical compartment in comparison to untreated cells, while showing similar Trp levels in the basolateral compartment for 1 μ M at 6 hours ($P < .01$) and for 3 μ M at 2 hours ($P < .05$) and 6 hours ($P < .01$). For 10 μ M Trp, this effect was found to be statistically significant at all time points ($P < .001$). In summary, these data suggested that addition of Trp led to either an inhibition of Trp secretion or an increased Trp uptake by the cells.

Transport studies with deuterated tryptophan

Since secretion of Trp complicated the analysis of Trp transport, we decided to apply deuterated Trp (dTrp) to study the transport mechanism in the oral mucosa model. The dTrp was applied at 10 and 100 μ M in HBSS for transport studies from the apical to the basolateral compartment (A/B) or from the basolateral to the apical (B/A) compartment with TEER values of $170 \pm 24.82 \Omega \times \text{cm}^2$ at the start of experiments. Samples were drawn on the opposite side after 30, 90, 210 and 450 minutes.

For determination of the permeability coefficients (PE) of 10 and 100 μ M dTrp from A/B or B/A, cleared volume (μL) over time was calculated for cells and blanks (ThinCerts without cells) and shown in Figure 2A and B. With slope values of cleared volume (μL) over time (min) under consideration of the area (cm^2), PE values ($\mu\text{m}/\text{min}$) from 0 to 30 minutes and 30 to 450 minutes were calculated for both directions. As a result, a significantly higher permeability from A/B ($1.44 \pm 0.31 \mu\text{m}/\text{min}$) than B/A ($0.89 \pm 0.22 \mu\text{m}/\text{min}$, $P < .001$) for the interval 0 to 30 minutes was determined for 10 μ M dTrp. For the interval of 30 to 450 minutes PE of $2.47 \pm 0.88 \mu\text{m}/\text{min}$ was calculated for A/B and $2.80 \pm 0.77 \mu\text{m}/\text{min}$ for B/A. Transport of 100 μ M dTrp led to PE values of $0.64 \pm 0.18 \mu\text{m}/\text{min}$ from A/B and $0.52 \pm 0.28 \mu\text{m}/\text{min}$ from B/A for 0 to 30 minutes and PE values from 30 to 450 minutes showed similar results as 10 μ M dTrp with $2.42 \pm 0.96 \mu\text{m}/\text{min}$ from A/B and $2.21 \pm 0.79 \mu\text{m}/\text{min}$ from B/A (Figure 2C).

To illustrate the difference of measured concentration from applied dTrp and secreted Trp over time, measured concentrations from the basolateral side of the A/B transport and concentrations from the apical side of the B/A transport of cells

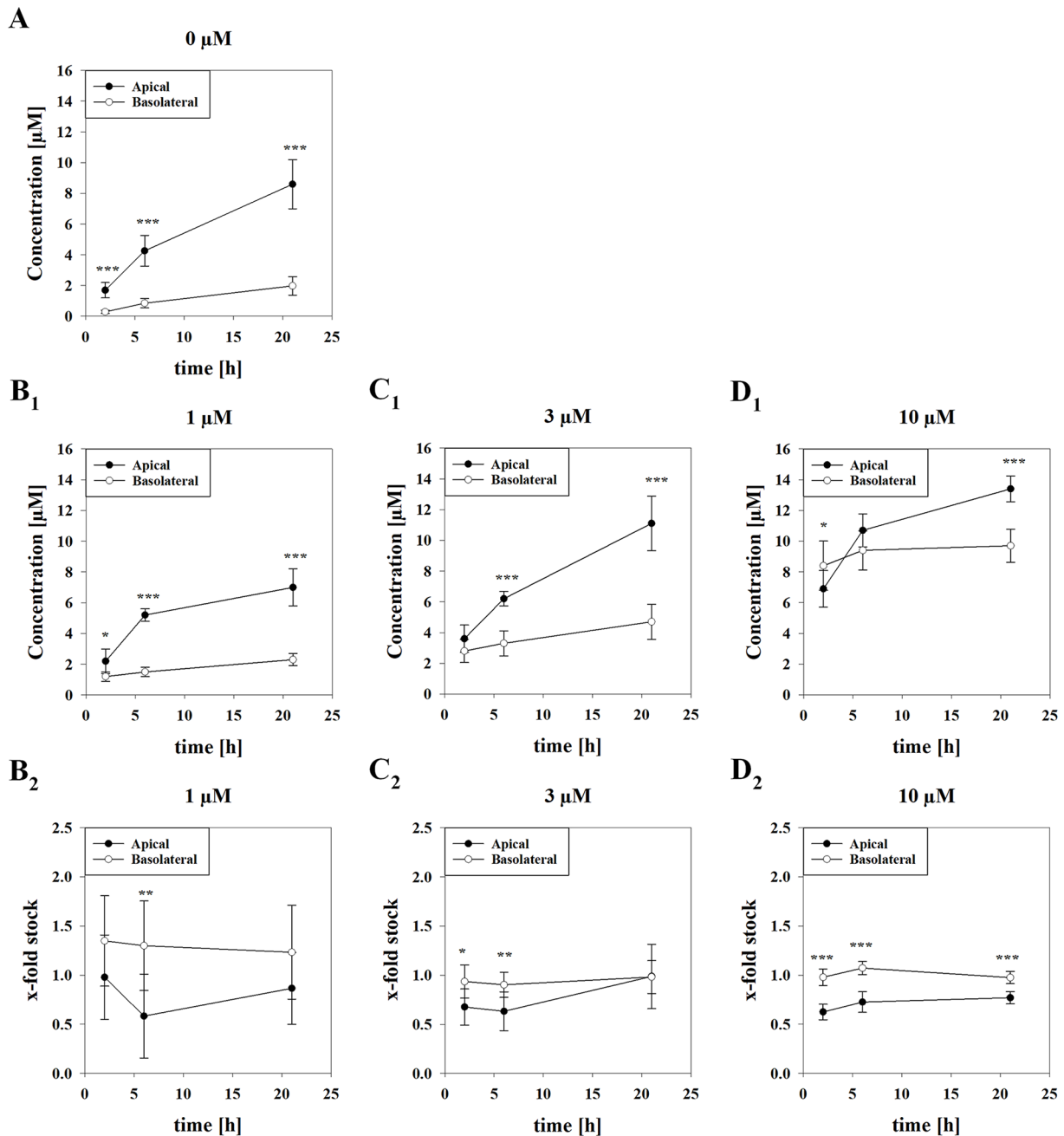


Figure 1. Measured tryptophan concentration on the apical and basolateral side upon treatment for 2, 6 and 21 hours with 0 μM (A), 1 μM (B₁), 3 μM (C₁) and 10 μM (D₁) tryptophan. Results shown as mean ± SD of 3 to 4 independent experiments (N=6-9). X-fold values referred to the applied stock solution upon subtraction of measured tryptophan concentration after treatment with 0 μM (A) for each timepoint shown for 1 μM (B₂), 3 μM (C₂) and 10 μM (D₂). Results shown as mean ± SD. Statistical analysis was performed as two-way ANOVA using post-hoc Holm-Sidak test with **P* < .05, ***P* < .01, ****P* < .001 and $\alpha = .05$ comparing measured apical concentration to measured basolateral concentration for each respective Trp concentration applied.

are displayed in Figure 2D and E. Respective Trp concentration values are plotted in Figure 2E. Permeated dTrp concentrations (μM) reflected the volume ratio between apical (300 μL) and basolateral compartment (900 μL), demonstrating a linear clearance over time for both applied concentrations, while similar levels of permeated Trp was measured for both applied dTrp concentrations to the basolateral and apical side. Finally, at the end of the transport studies with dTrp rather similar concentrations of unlabeled Trp were found in the apical (A/B: $5.23 \pm 1.54 \mu\text{M}$ Trp [10 μM dTrp]; $4.59 \pm 1.65 \mu\text{M}$ Trp [100 μM dTrp]) as well as in the

basolateral compartment (B/A: $1.33 \pm 0.22 \mu\text{M}$ Trp [10 μM dTrp]; $2.22 \pm 0.20 \mu\text{M}$ Trp [100 μM dTrp]) compared to the previous experiments and confirmed the reduced Trp concentration at the apical side at higher dTrp concentrations.

Regulation of LAT1 by BCH and L-leucine and changed mRNA expression upon exposure to tryptophan

Trp, a neutral amino acid, is transported by the Na⁺- and pH-independent L-type amino acid transporter 1 (LAT1),²⁰ which

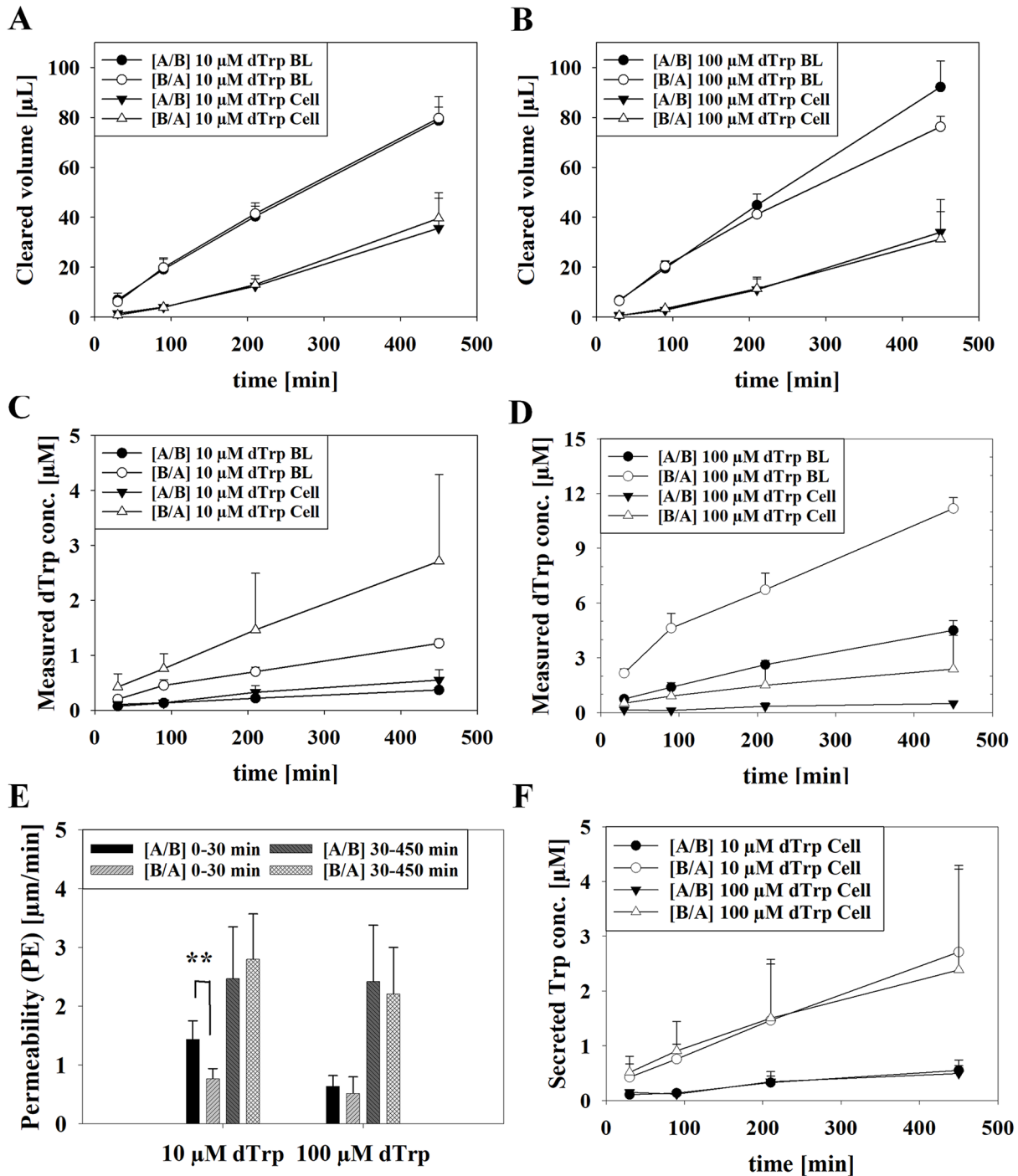


Figure 2. (A, B) Measured clearance (μL) of blanks (BL) compared to cells (Cell) upon applying $10\ \mu\text{M}$ (A) and $100\ \mu\text{M}$ dTrp (B) from the apical to the basolateral (A/B) or B/A for each time point (30, 90, 210 and 450 minutes) and (C, D) corresponding measured dTrp concentration. (E) Calculated permeability (PE) values ($\mu\text{m}/\text{min}$) of transport studies with 10 and $100\ \mu\text{M}$ deuterated Trp (dTrp) applied from the A/B compartment or vice versa (B/A) after 0 to 30 minutes or 30 to 450 minutes. Statistical analysis was performed as Student's *t*-test with $**P < .01$ and $\alpha = .05$. (F) Secreted Trp during transport studies with $10\ \mu\text{M}$ dTrp and $100\ \mu\text{M}$ dTrp. Results shown as mean \pm SD from 2 independent experiments ($N=6$).

has previously been shown to be expressed in oral carcinoma cells.^{21,22} Immunofluorescence staining confirmed the ubiquitous expression of LAT1 in our model based on TR146 cells cultivated on microscope slides and on ThinCerts (Figure 3A). To examine the influence of media on LAT1 expression, Western blotting was performed on samples of cells treated with DMEM without serum and HBSS for 24 hours

compared to cells cultivated in media with serum (Figure 3B). Densitometric analysis of Western blots revealed no significant differences between cells treated with media without serum (0.77 ± 0.29 , $P = .44$) or cells treated with HBSS (1.10 ± 0.07 , $P = .37$) in comparison to control (media with serum, 1.00 ± 0.10) indicating that the expression of LAT1 was not changed by the application of HBSS itself.

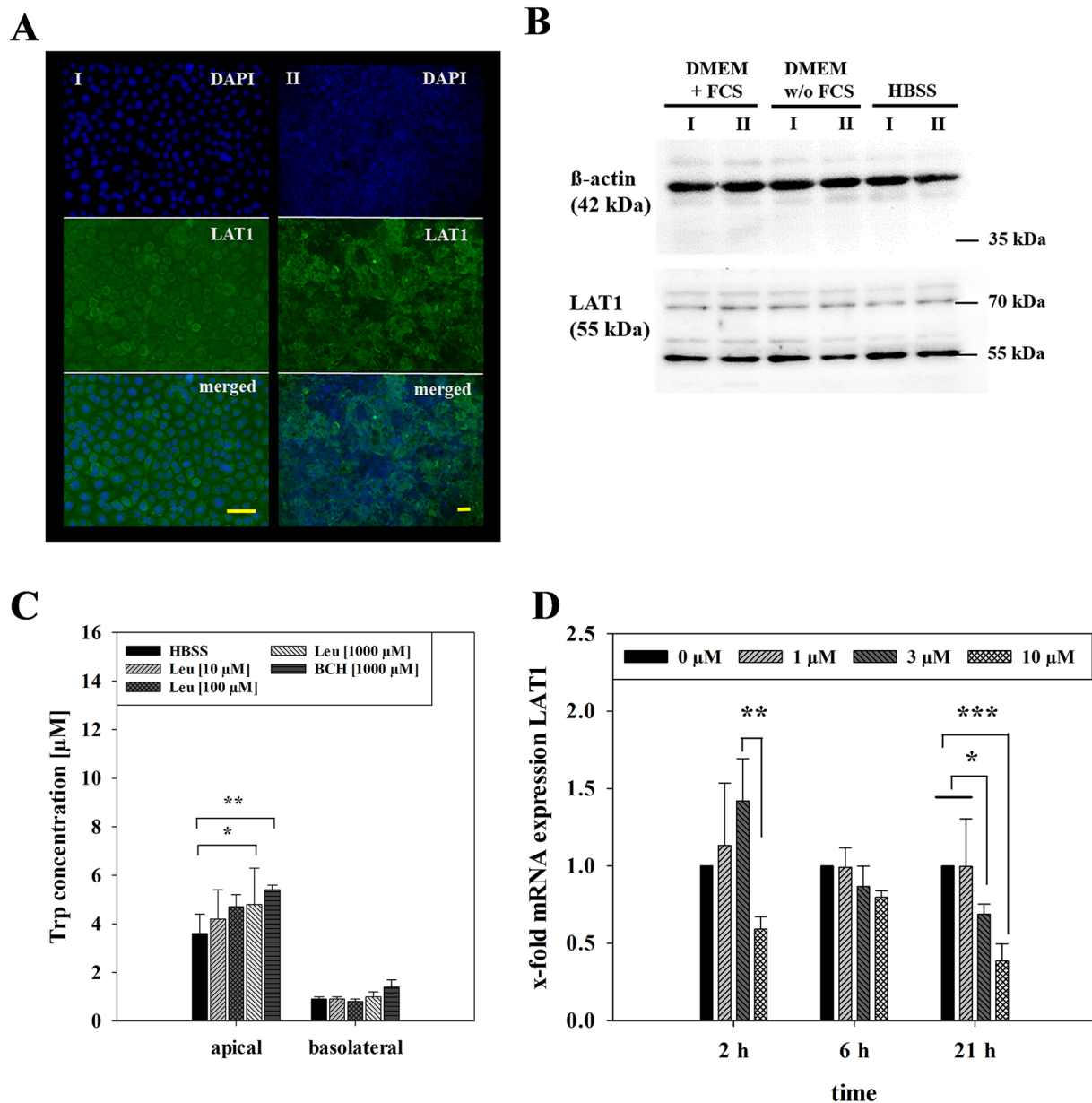


Figure 3. (A) Immunofluorescence staining for LAT1 and DAPI of TR146 seeded on microscopic slides (I, 20× magnification) and of TR146 seeded on 24-well ThinCerts (II, 10× magnification), yellow scale bar represents 50 μm. (B) Western blot of LAT1 and endogenous control β-actin of TR146 in DMEM supplemented with 10% FCS and 1% Pen/Strep compared to TR146 treated for 24 hours in DMEM without FCS (supplemented with 1% Pen/Strep) and HBSS of 2 independent experiments (I, II); (C) measured Trp concentration upon 6 hours incubation with L-leucine (10, 100, 1000 μM) and BCH (1000 μM) compared to HBSS on the apical and basolateral side. Shown as mean ± SD of 1 to 2 independent experiments (N=3-8). Statistical analysis was performed as two-way ANOVA using post-hoc Holm-Sidak test with * $P < .05$, ** $P < .01$, *** $P < .001$ and $\alpha = .05$. (D) mRNA expression of LAT1 after equilibrium studies with 1, 3 and 10 μM Trp for 2, 6 and 21 hours from 2 to 4 independent experiments (N=2-3). Results displayed as x-fold to 0 μM (control) upon normalization to endogenous control (18S rRNA) and calculated as mean ± SD. Statistical analysis was performed as three-way ANOVA with * $P < .05$, ** $P < .01$, *** $P < .001$ and $\alpha = .05$.

For evaluation of the functional activity of LAT1 in our model, BCH and L-leucine (Leu) were applied at 10, 100 or 1000 μM in HBSS on the apical and basolateral side (Figure 3C). Measurements after 6 hours showed significantly increased Trp concentration on the apical side for treatment with 1000 μM Leu ($4.78 \pm 1.55 \mu\text{M}$, $P < .05$) and 1000 μM BCH ($5.44 \pm 0.16 \mu\text{M}$, $P < .01$) compared to HBSS alone ($3.64 \pm 0.82 \mu\text{M}$) while basolateral concentrations of Trp showed no significant difference

(1000 μM Leu: $1.05 \pm 0.20 \mu\text{M}$, $P = .99$; 1000 μM BCH: $1.42 \pm 0.32 \mu\text{M}$, $P = .93$; HBSS: $0.88 \pm 0.15 \mu\text{M}$). This indicated that LAT1 inhibition led to increased Trp in the apical compartment, suggesting a role for apical LAT1 in Trp uptake.

To analyse the effect of treatment with Trp on LAT1 at the mRNA level, qPCRs for LAT1 were performed with 18S rRNA as endogenous control. In equilibrium studies ΔCt values of samples treated with Trp were normalized to ΔCt values of

control samples (treated with 0 μM Trp) at each timepoint (Figure 3D) to analyse the regulation over time. After 2 hours, 10 μM Trp led to a significantly reduced expression of LAT1 (0.60 ± 0.08) in comparison to 3 μM Trp (1.42 ± 0.27 , $P < .01$). While 6 hours treatment showed no significant regulation by applied Trp, treatment for 21 hours with 3 and 10 μM Trp led to significantly downregulated expression of LAT1 with 0.69 ± 0.07 for 3 μM ($P < .05$) and 0.39 ± 0.11 for 10 μM ($P < .001$) in comparison to 0 μM Trp (1 ± 0) or 1 μM Trp (1.00 ± 0.31). Similar to this, addition of dTrp also caused LAT1 downregulation upon treatment with 10 or 100 μM dTrp in transport studies in comparison to LAT1 expression at the start of the experiments ($P < .05$ for 10 μM dTrp A/B and 100 μM dTrp A/B, B/A; Figure S2). These findings supported the concept that LAT1 is involved in Trp uptake on the apical side and may be downregulated when there is an excess of Trp available.

Discussion

Trp plays an important role in regulation of inflammation due to its metabolism down the kynurenine pathway. As changes of Trp levels in body fluids have been linked to diseases, a non-invasive determination of Trp concentration in for example, saliva offers advantages for diagnosis or monitoring of a disease.

The here reported equilibrium studies with Trp using an oral mucosa epithelium *in vitro* model showed secretion of Trp by TR146 cells treated with amino-acid free buffer and moreover a decrease of Trp concentration upon exposure to additional Trp on the apical side, suggesting the involvement of a saturable transport system (Figure 1). Prior to equilibrium studies with Trp, preliminary studies were performed with cells washed weekly with an amino-acid free buffer on the apical side and compared to cells washed with the buffer only on day of experiment. This was accomplished to exclude that the found increased Trp concentration on the apical side might origin from the previous interaction/adsorption of serum components with the apical cell surface. Treatment with amino-acid-free buffer and 3 μM Trp for 2, 6 and 21 hours showed no consistent increase or decrease of Trp concentration in the apical or basolateral side comparing apically washed and non-washed cells and excluded an influence of serum during the cultivation before the experiments on transport of Trp (data not shown). Corresponding to our results demonstrating higher apical Trp concentrations when no external Trp was added, previous clinical studies showed a significant increase of free Trp after its depletion.²³ Additionally, higher Trp levels were measured in oral squamous tissue of cancer patients in comparison to control tissue in a preliminary study,²⁴ which was explained by the upregulated expression of the sodium and pH-independent neutral amino acid transporter LAT1 in several types of cancer, necessary for providing nutrients for growth.^{9,25}

The dTrp was used for transport studies and administered on the apical or basolateral side with samples drawn at multiple time points to evaluate the effective transport direction of the amino acid itself. Results showed a significantly higher permeability from the apical to the basolateral compartment after 30 minutes upon applying 10 μM dTrp (Figure 2). The applied cell culture model in our study was validated for its suitability for directed transport studies by performing permeability assays with the paracellular marker molecule carboxyfluorescein from the apical to the basolateral side or from the basolateral to the apical side previously, resulting in no preference for a transport direction for the paracellular marker.¹⁵ Hence, an increased permeability from the apical (saliva) to the basolateral (blood) compartment suggested a directed transcellular transport for dTrp at this concentration and the applied time window. In future investigations, lower dTrp concentrations at shorter time frames could be used to investigate the mechanistic details of Trp transport. A previous study by Geisler et al. with volunteers reported a concentration of $1.48 \pm 3 \mu\text{M}$ Trp in saliva and $65 \pm 10 \mu\text{M}$ Trp in serum (mean \pm SD, $n=151$), suggesting that Trp transport across the blood-saliva barrier is limited to the serum unbound Trp fraction.²⁶ Furthermore, a preliminary study investigating patients ($n=4$) with oral squamous cell carcinoma and their Trp level in saliva, serum, healthy and cancerous tissue, reported a Trp concentration of $3.81 \pm 0.62 \mu\text{M}$ in saliva and $33.73 \pm 2.52 \mu\text{M}$ in serum while observing higher Trp concentration in cancerous tissue ($30.21 \pm 5.88 \mu\text{M}$) compared to healthy one ($13.28 \pm 0.62 \mu\text{M}$).²⁴ These data also indicated an increased uptake of Trp in cancer cells possibly mediated by increased LAT1 function.^{9,25} In this regard, the expression of LAT1 was confirmed in our oral mucosa model by immunofluorescence staining (Figure 3) coinciding with previously published results.²⁷ BCH, an inhibitor for LAT1 and LAT2, has shown to inhibit L-Leu and L-Trp influx regulated by LAT1 in a concentration dependent manner in cancer cells.^{28,29} Furthermore, addition of Leu in animal studies with mice has shown to decrease the ratio of Kyn to Trp in the plasma to brain ratio.³⁰ Treating our model with BCH and Leu for 6 hours increased Trp levels in the apical compartment, suggesting a cellular uptake of Trp partly mediated by LAT1 in our model.

LAT1 expression was also investigated in response to Trp exposure. Our findings showed significantly reduced expression of LAT1 after equilibrium studies over time correlating to the applied Trp concentration (Figure 3), indicating a concentration dependent downregulation of LAT1. Furthermore, slightly significantly reduced expression of LAT1 was observed after transport as well (Figure S2). As literature described LAT1 to form a heterodimeric complex with 4F2hc (also known as SLC3A2), a membrane glycoprotein,⁹ qPCR was performed with a primer for 4F2hc described by Zhu et al³¹ after equilibrium studies (data not shown). However, no distinct regulation of the glycoprotein was shown in our model in accordance to findings published by Napolitano et al, stating

LAT1 to be the sole transport unit of the complex.³² As previous studies demonstrated an upregulation of 4F2hc after treatment with LPS but no regulation of LAT1,³⁰ lack of regulation of 4F2hc may indicate no harmful effect on our cells by applying HBSS during the experiments. To monitor for possible detrimental effects of HBSS incubation on our model during the experimental duration, LDH assay was performed after 6 and 21 hours showing similar viability values for both time points (Figure S3), demonstrating no cytotoxic effect of HBSS on the viability over time.

In summary, our findings demonstrated Trp secretion in our oral mucosa epithelium model and suggested a role of LAT1 for apical uptake of Trp supported by data obtained after addition of Trp, BCH and Leu. The apical function of LAT1 could partly also contribute to the preferred transport direction of dTrp from the apical (saliva) to the basolateral (blood) compartment. These findings could contribute to explain the limited Trp concentration in saliva, as reported by Geisler et al, who compared the Trp levels of 151 healthy subjects (mean \pm SD) in saliva ($1.48 \pm 3.00 \mu\text{M}$ Trp) and blood ($65 \pm 3.0 \mu\text{M}$ Trp), besides the assumed limitation that only free Trp can pass the epithelial barrier.²⁶ In addition, it should be considered that the methodology of saliva sampling has an influence on the result obtained, as saliva is produced by several major salivary glands, which contribute to a different composition of saliva depending on the stimulus. It is therefore important to define and establish a sampling protocol before performing saliva diagnostics in order to obtain comparable results.

Future studies could include further analysis of the functionality of the LAT1 transporter, for example by treatment with siRNA or by applying other ligands for the transporter system. Involvement of further amino acid transporters such as LAT2 needs further investigations to understand the transport of Trp and possible counter regulations. Moreover, additional studies regarding the transport direction of Trp for example, across salivary gland epithelia models are necessary to further estimate the usability of Trp as a salivary biomarker. In addition, the impact of the oral microbiome or periodontal inflammatory processes need to be considered when trying to establish Trp as a salivary biomarker.^{33,34}

Acknowledgements

Special thanks to Tamara Leitgeb for her assistance during the first part of the practical work.

Author Contributions

GCL: Conceptualization, methodology, formal analysis, investigation, writing - original draft preparation, writing - review and editing, visualization, project administration. JT: Investigation, formal analysis, validation. LM: Investigation, formal analysis, validation. H-PF: Investigation. DF: Formal

analysis, validation, writing - review and editing. TF: Investigation, formal analysis, validation, writing - review and editing. JMG: Investigation, formal analysis, validation, writing - review and editing. WN: Conceptualization, methodology, formal analysis, resources, writing - original draft preparation, writing - review and editing, supervision, project administration, funding acquisition.

Supplemental Material

Supplemental material for this article is available online.

REFERENCES

- Platten M, Nollen EAA, Röhrig UF, Fallarino F, Opitz CA. Tryptophan metabolism as a common therapeutic target in cancer, neurodegeneration and beyond. *Nat Rev Drug Discov.* 2019;18:379-401.
- Höglund E, Øverli Ø, Winberg S. Tryptophan metabolic pathways and brain serotonergic activity: a comparative review. *Front Endocrinol (Lausanne).* 2019;10:158.
- Sorgdrager FJH, Naudé PJW, Kema IP, Nollen EA, Deyn PP De. Tryptophan metabolism in inflammaging: from biomarker to therapeutic target. *Front Immunol.* 2019;10:2565.
- Sofia MA, Ciorba MA, Meckel K, et al. Tryptophan metabolism through the kynurenine pathway is associated with endoscopic inflammation in ulcerative colitis. *Inflamm Bowel Dis.* 2018;24:1471-1480.
- Nikolaus S, Schulte B, Al-Massad N, et al. Increased tryptophan metabolism is associated with activity of inflammatory bowel diseases. *Gastroenterology.* 2017;153:1504-1516.e2.
- Cussotto S, Delgado I, Anesi A, et al. Tryptophan metabolic pathways are altered in obesity and are associated with systemic inflammation. *Front Immunol.* 2020;11:557.
- Porter RJ, Lunn BS, Walker LL, Gray JM, Ballard CG, O'Brien JT. Cognitive deficit induced by acute tryptophan depletion in patients with Alzheimer's disease. *Am J Psychiatry.* 2000;157:638-640.
- Willette AA, Pappas C, Hoth N, et al. Inflammation, negative affect, and amyloid burden in Alzheimer's disease: insights from the kynurenine pathway. *Brain Behav Immun.* 2021;95:216-225.
- Yan R, Zhao X, Lei J, Zhou Q. Structure of the human LAT1-4F2hc heteromeric amino acid transporter complex. *Nature.* 2019;568:127-130.
- Scalise M, Galluccio M, Console L, Pochini L, Indiveri C. The human SLC7A5 (LAT1): the intriguing histidine/large neutral amino acid transporter and its relevance to human health. *Front Chem.* 2018;6:243.
- Häfliger P, Charles R-P. The L-type amino acid transporter LAT1-an emerging target in cancer. *Int J Mol Sci.* 2019;20:2428.
- Yoshizawa JM, Schafer CA, Schafer JJ, Farrell JJ, Paster BJ, Wong DTW. Salivary biomarkers: toward future clinical and diagnostic utilities. *Clin Microbiol Rev.* 2013;26:781-791.
- Pay JB, Shaw AM. Towards salivary C-reactive protein as a viable biomarker of systemic inflammation. *Clin Biochem.* 2019;68:1-8.
- Lin GC, Leitgeb T, Vladetic A, et al. Optimization of an oral mucosa in vitro model based on cell line TR146. *Tissue Barriers.* 2020;8:1748459.
- Lin GC, Küng E, Smajlhodzic M, et al. Directed transport of CRP across in vitro models of the blood-saliva barrier strengthens the feasibility of salivary CRP as biomarker for neonatal sepsis. *Pharmaceutics.* 2021;13:256.
- Lin GC, Smajlhodzic M, Bandian A-M, et al. An in vitro barrier model of the human submandibular salivary gland epithelium based on a single cell clone of cell line HTB-41: establishment and application for biomarker transport studies. *Biomedicines.* 2020;8:302.
- Laich A, Neurauter G, Widner B, Fuchs D. More rapid method for simultaneous measurement of tryptophan and kynurenine by HPLC. *Clin Chem.* 2002;48:579-581.
- Widner B, Werner ER, Schennach H, Wachter H, Fuchs D. Simultaneous measurement of serum tryptophan and kynurenine by HPLC. *Clin Chem.* 1997;43:2424-2426.
- Fuertig R, Ceci A, Camus SM, Bezard E, Luippold AH, Hengerer B. LC-MS/MS-based quantification of kynurenine metabolites, tryptophan, monoamines and neopterin in plasma, cerebrospinal fluid and brain. *Bioanalysis.* 2016;8:1903-1917.
- Prasad PD, Wang H, Huang W, et al. Human LAT1, a subunit of system L amino acid transporter: molecular cloning and transport function. *Biochem Biophys Res Commun.* 1999;255:283-288.

21. Zhao Y, Wang L, Pan J. The role of L-type amino acid transporter 1 in human tumors. *Intractable Rare Dis Res.* 2015;4:165-169.
22. Yun D, Lee SA, Park M, et al. JPH203, an L-type amino acid transporter 1 – selective compound, induces apoptosis of YD-38 human oral cancer cells. *J Pharmacol Sci.* 2014;217:208-217.
23. Porter RJ, Gallagher P, O'Brien JT. Effects of rapid tryptophan depletion on salivary cortisol in older people recovered from depression, and the healthy elderly. *J Psychopharmacol.* 2007;21:71-75.
24. Tankiewicz A, Dziemiańczyk D, Buczek P, Szarmach IJ, Grabowska SZ, Pawlak D. Tryptophan and its metabolites in patients with oral squamous cell carcinoma: preliminary study. *Adv Med Sci.* 2006;51 Suppl 1:221-224.
25. Geier EG, Schlessinger A, Fan H, et al. Structure-based ligand discovery for the Large-neutral Amino Acid Transporter 1, LAT-1. *Proc Natl Acad Sci USA.* 2013;110:5480-5485.
26. Geisler S, Gostner JM, Schnell T, Fuchs D. Measurements of neopterin and aromatic amino acids in saliva. 36th International Winter Workshop Clinical, Chemical and Biochemical Aspects of Pteridines and Related Topics. *Pteridines.* 2017;28:37-58.
27. Kim DK, Ahn SG, Park JC, Kanai Y, Endou H, Yoon JH. Expression of L-type amino acid transporter 1 (LAT1) and 4F2 heavy chain (4F2hc) in oral squamous cell carcinoma and its precursor lesions. *Anticancer Res.* 2004;24:1671-1675.
28. Kim CSK, Ho SC, Hun SC, Ee SL, Ndou HE. BCH, an inhibitor of system L amino acid transporters, induces apoptosis in cancer cells. *Biol Pharm Bull.* 2008;31:1096-1100.
29. Travers MT, Gow IF, Barber MC, Thomson J, Shennan DB. Indoleamine 2, 3-dioxygenase activity and L-tryptophan transport in human breast cancer cells. *Biochim Biophys Acta.* 2004;1661:106-112.
30. Walker AK, Wing EE, Banks WA, Dantzer R. Leucine competes with kynurenine for blood-to-brain transport and prevents lipopolysaccharide-induced depression-like behavior in mice. *Mol Psychiatry.* 2019;24:1523-1532.
31. Zhu B, Cheng D, Hou L, Zhou S, Ying T, Yang Q. SLC3A2 is upregulated in human osteosarcoma and promotes tumor growth through the PI3K/Akt signaling pathway. *Oncol Rep.* 2017;37:2575-2582.
32. Napolitano L, Scalise M, Galluccio M, Pochini L, Albanese LM, Indiveri C. LAT1 is the transport competent unit of the LAT1/CD98 heterodimeric amino acid transporter. *Int J Biochem Cell Biol.* 2015;67:25-33.
33. Leblhuber F, Steiner K, Geisler S, Fuchs D, Gostner JM. On the possible relevance of bottom-up pathways in the pathogenesis of Alzheimer's disease. *Curr Top Med Chem.* 2020;20:1415-1421.
34. Kurgan Ş, Önder C, Balcı N, et al. Influence of periodontal inflammation on tryptophan-kynurenine metabolism: a cross-sectional study. *Clin Oral Investig.* 2022;26:5721-5732.